PCCP

Accepted Manuscript




ROYAL SOCIETY OF CHEMISTRY

www.rsc.org/pccp

# Sensing the Quantum Behaviour of Magnetic Nanoparticles by Electron Magnetic Resonance

M. Fittipaldi[1*], R. Mercatelli[1], S. Sottini[2], P. Ceci[3], E. Falvo[3,4], D. Gatteschi[2]

[1]*INSTM and Department of Physics and Astronomy, University of Florence, via Sansone 1, 50019 Sesto Fiorentino, Italy*

[2]*INSTM and Department of Chemistry "U. Schiff," University of Florence, via della Lastruccia, 3-13 50019 Sesto Fiorentino, Italy*

[3]*CNR, Institute of Molecular Biology and Pathology, 00185 Rome, Italy*

[4]*Department of Biochemical Sciences "A. Rossi Fanelli", University "Sapienza", Rome, Italy*

[*]Corresponding author: maria.fittipaldi@unifi.it

## Abstract

We have investigated Magnetic Nanoparticles (MNPs) of spinel type iron oxide (of approximately 8 nm) mineralized in the internal cavity of the bioreactor ferritin nanocage. In particular, we have used Electron Magnetic Resonance, EMR, spectroscopy and taken advantage of the capacity of the protein shells to control the size of the MNP. EMR measurements in perpendicular and parallel configurations have been recorded at various temperature. A model based on the giant spin is used to interpret the experimental results. The analysis indicates that the observed quantum behaviour has to be ascribed to the whole MNP and that the thermal population of excited spin states has a strong influence in the EMR behaviour of MNPs.

## Introduction

The study of nanomagnetic systems has received considerable attention in recent years, driven by both fundamental scientific interest[1,2] and potential technological applications[3-10,10-14]. The key significance of such systems derives from the emergence of new properties imposed by the reduced dimensions. Two classes of zero-dimensional magnetic objects may be distinguished, magnetic nanoparticles (MNPs), which can be considered to be derived from a top down approach, and molecular nanomagnets (MNMs), which are obtained through molecular techniques in a bottom up approach. Theoretically, MNMs are described by quantum mechanics, with a treatment that starts from the single ion, while MNPs are described classically, based on parameters derived from bulk materials. The need for a unified view of such systems has been proposed, which may provide

greater insight into their properties.[1,15] The promise offered by this approach, by comparing the magnetic behaviour of the two classes of systems, has already shown fruitful results. In particular, Electron Magnetic Resonance (EMR) has been a key tool in demonstrating the similarities in the behaviour of MNPs and MNMs, enabling recognition of the experimental signature of quantum behaviour in small MNPs.[16-18] Indeed, some evidence has been collected regarding the discrete nature of the spin levels of these systems by the observation of a half-field signal in the EMR spectra of small MNPs.

We have investigated MNPs of spinel type iron oxide, of approximately 8 nm, mineralized in the internal cavity of the bioreactor ferritin. In particular, we have used EMR spectroscopy and taken advantage of the capacity of the protein shells of ferritin from the hyperthermophilic archaeon *Pyrococcus furiosus* (PfFt) to control the size and the iron oxide phase of the MNPs, using an approach that has been previously exploited.[16] The MNPs thus formed in the protein cages are constituted by 4000 Fe ions, in the form of maghemite/magnetite.

In an attempt to investigate further the quantum nature of small MNPs, EMR spectra were recorded in both parallel and perpendicular configuration, *i.e.* with the $B_1$ field of the microwave radiation parallel and perpendicular to the external $B_0$ field. These alternative measurement configurations have different selection rules for the allowed transitions between the total spin projections; therefore, this provides a means to sense and address the quantum nature of the system.

The simulation of the EMR data reported herein represents an important step forward. The EMR spectra of MNPs in PfFt have been interpreted using an approach based on the giant spin model to describe the interaction of their ground spin state with the external magnetic field, similar to the approach successfully employed for MNMs.[19-23] However, for MNPs, there is a strong drawback: the ground spin state of MNPs is estimated to be of the order of thousands, taking into account that the structural disorder in MNPs propagates from the surface towards the interior for a distance of approximately one nm.[24] If one starts from the naïve estimation that the total spin derives from the ferromagnetic coupling of 4000 Fe(III) ions each of spin 5/2, a total spin of the order of $10^4$ would be derived. Therefore, a full matrix diagonalization of the spin Hamiltonian is impossible given the dimension of the Hilbert space. However, there are experimental observations that may indicate the way to follow. In the EMR spectra of MNPs the fine structure signature is absent. Instead, this was readily observed in the high field-high frequency electron paramagnetic resonance (EPR) spectra of small MNMs;[20] it is absent in the powder spectra of large MNMs, though it may still be partially resolved in single crystal high field EPR.[25] These observations prompted us to develop a simplified simulation approach that made use of an effective smaller spin value and, accordingly, effective spin Hamiltonian and experimental parameters. This simplified

approach has highlighted clearly that the half-field contributions to the spectra, enhanced when the spectra are recorded in parallel configuration, derive from the whole system; hence, the corresponding energy levels must be discrete. Moreover, the EMR data acquired in both configurations and the simulation approach followed indicate that the temperature dependence of the spectra is strongly influenced by thermal population of excited spin states. This will be discussed in comparison with the trend observed for MNMs.

## Materials and methods

**EMR Spectroscopy**. X-band EMR measurements were performed using the 9 GHz Bruker Elexys E500 instrument (Bruker, Rheinstetten, Germany) equipped with a microwave frequency counter. An Oxford Instruments ESR 900 continuous He flow cryostat was used to obtain low temperatures. EPR spectra were acquired using a field modulation of 100 kHz and 5 G, and a microwave power of 26 μW for the perpendicular configuration and 21 mW for the parallel configuration. The ER 4116DM EPR-resonator (Bruker, Rheinstetten, Germany) was used for the measurements.

**MNP synthesis in PfFt proteins.** Apo-PfFt protein was expressed and purified as reported elsewhere.[26] MNPs were encapsulated inside the PfFt nanocage as previously reported by ourselves, with minor modifications.[16] Briefly, MNPs were prepared at 65 °C at 1 mg/mL protein concentration in 5 mM HEPES-NaOH (Sigma Aldrich, Italy) pH of 8.5. Solutions of iron(II) sulfate heptahydrate (Sigma Aldrich, Italy), dissolved in 0.5 mM HCl were used as an iron source. During the synthesis the reaction vessel was kept at 65°C under a positive $N_2$ pressure and the pH was actively maintained at 8.5 with 100 mM NaOH by means of an automatic titrator (TITRANDO, Metrohm AG). Solutions of $FeSO_4$ (15 mM) and $H_2O_2$ (5 mM) were added simultaneously at a constant rate of 0.5 mL/min using two automatic titrators of the TITRANDO system (software TIAMO$^{tm}$). Any aggregate of protein or metal oxides produced outside the protein cavity during NP formation was removed by centrifugation at 16000 rpm for 45 min. at 4°C, followed by filtration through 0.2 μm filters. Subsequently, the NP solutions were ultrafiltrated and washed 3 times with phosphate buffered saline (PBS) by using 100 kDa Amicon Ultra-15 centrifugal filter devices (Millipore Corporate) to remove excess reagents. The PfFt samples were filtered in a sterile way and stored at 4 °C. MNP samples had a loading factor of about 4000 metal atoms/protein molecule, as assessed by means of native electrophoresis on 1% agarose gels and use of the ferrozine method as described in Ceci *et al*.[17]

**Results**

EMR spectra of MNPs mineralized in the internal cavity of *P. furiosus* ferritin have been acquired at X-band both in perpendicular and parallel configuration at various temperatures (Figures 1 and 2). It is evident that upon lowering the temperature the EMR spectra of MNPs acquired in the perpendicular configuration, become broader and the resonance position ($B_0$) shifts towards lower field values. This can be qualitatively explained by considering that upon decreasing the temperature, the MNP changes gradually from a system displaying superparamagnetic behaviour to one in which the magnetic fluctuations are blocked, with the anisotropy field of the MNP becoming more effective in influencing the resonance position. As a result, the spectra become broader and the resonance position shifts towards lower field values. The peak to peak intensity decreases but clearly not the double integral of the EMR spectra. Moreover, at high temperatures, a smaller band at $B_0/2$ *(around 1700 G)* is also observed, which has been attributed to 'partially' forbidden transitions between states with $\Delta M = \pm 2$, where M is the expectation value of $\hat{S}_z$ and S the total spin of the MNP.[16,18] If this interpretation is correct, the intensity of the $B_0/2$ signal must increase when the EMR spectra are recorded in the parallel configuration. The EMR experiments performed in this configuration have confirmed that this is the case (Figure 2); the intensity of the transitions at half field are clearly observed to increase. In addition, even bands at lower field values, deriving from $\Delta M = \pm 3$ and $\Delta M = \pm 4$ transitions, also become visible. Moreover, a rather marked temperature dependence of the EMR spectra acquired in parallel configuration is observed.

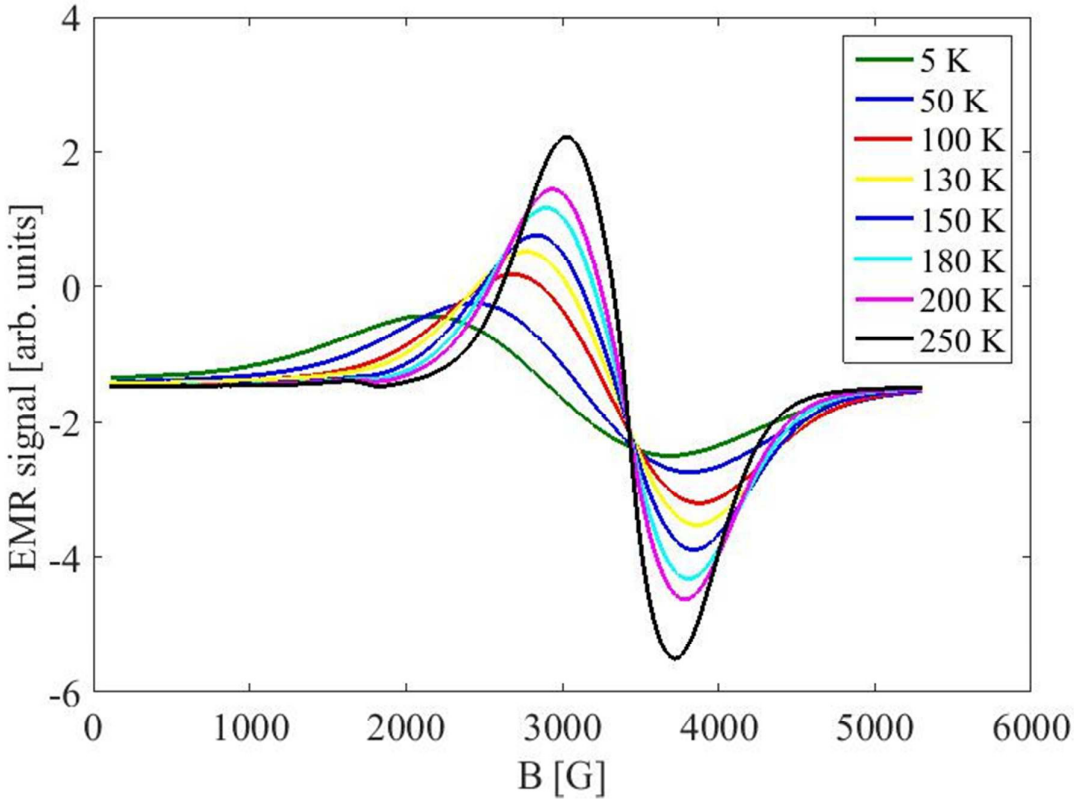


***Figure 1**: EMR spectra of MNPs in ferritin acquired at X-band in perpendicular configuration at various temperatures. The microwave frequency used was 9.64 GHz.*

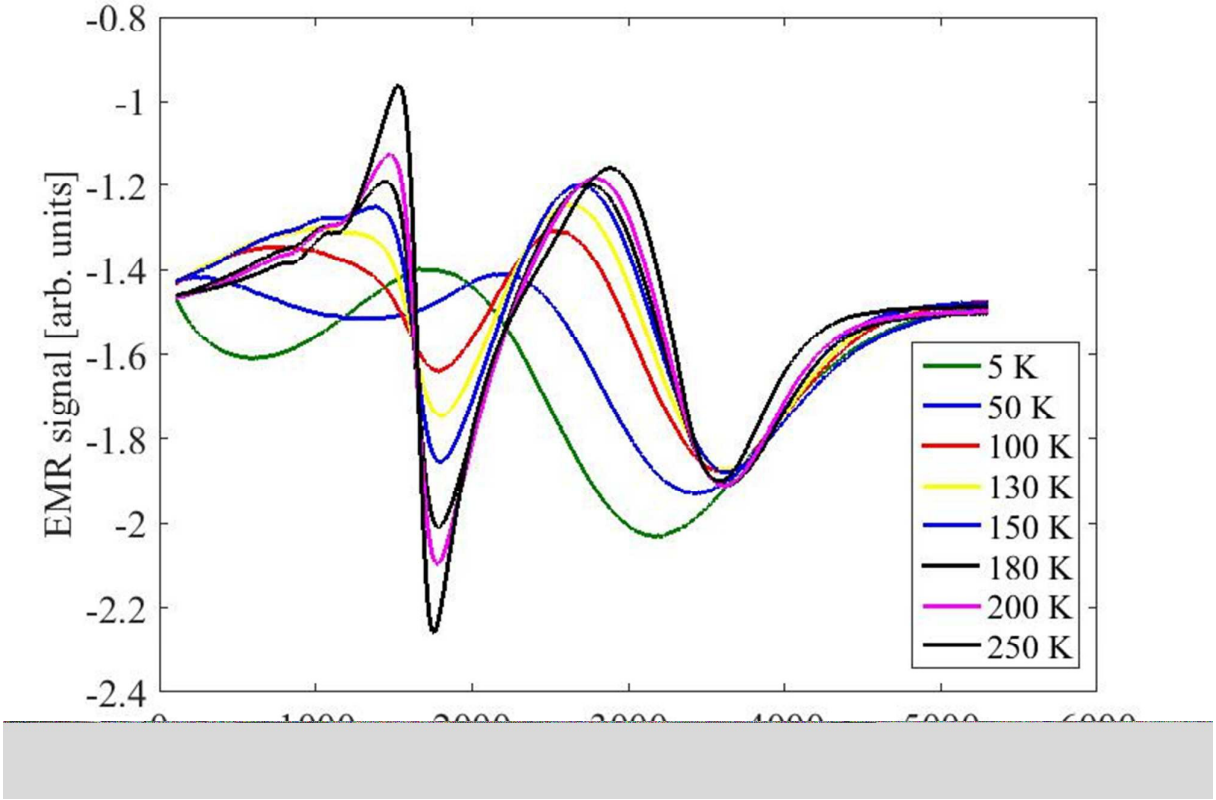


***Figure 2****: EMR spectra of MNPs in ferritin acquired at X-band in parallel configuration at various temperatures. The microwave frequency used was 9.40 GHz*

**Theoretical Model**

In an attempt to investigate further the quantum nature of these systems, the EMR spectra of the MNPs were interpreted using a model based on the giant spin associated with the whole MNP to describe the interaction of its ground spin state with the external magnetic field, similar to the approach successfully followed for MNMs. In particular, from previously reported magnetic measurements,[16] the saturation magnetization (obtained at 1.8 K) and the anisotropy field were found to be *71.4 emu/g* and *1.4 T*, respectively. The magnetic moment of each MNP is equal to $M_S V_p$, where $M_S$ is the volume magnetization of *357 emu/cm*$^3$, obtained assuming that the density of maghemite or magnetite is 5g/cm$^3$, and $V_p$ the particle volume assuming a particle radius of 4 nm.

From the relation $S = \frac{\mu}{g\mu_B}$, the ground state spin value of the MNP can be estimated to be of the order of 5000. By use of the relation $D = -\frac{\gamma B_a}{2S}$ together with the known value of the anisotropy field ($B_a$) and the estimated S value, a D value of -0.4 MHz ($-1.2 \cdot 10^{-5}$ cm$^{-1}$) is obtained.

However, given the spin value of the ground state, a full matrix diagonalization of the spin Hamiltonian is impossible. The absence of fine structure in the EMR spectra of MNPs, due to the small value of D, prompted us to develop a simplified simulation approach for MNPs, which makes use of an effective smaller spin value.

The basis of this simplified simulation approach is that the EMR spectrum of a MNP of spin S can be simulated using an effective lower spin $S_{eff} = \frac{S}{n}$ (with n integer and positive), provided that the DS value is kept constant such that $B_a$ also remains constant. Consequently, an effective D value has to be used $D_{eff}$= nD. In order to have equivalent EMR spectra for the real and effective systems, the temperature has to be scaled accordingly in order to compare the thermal energy $k_BT$ with $DS^2$, which is the energy barrier of the system. Therefore, in order to simulate at an experimental temperature T, an effective temperature of $T_{eff} = \frac{T}{n}$ has to be used for the effective spin system.

The spin Hamiltonian used for the system is

$$H = \mu_B \hat{S} \cdot g \cdot \vec{B} + \hat{S} \cdot D \cdot \hat{S} \quad (1)$$

the first term is the Zeeman term, the second is the zero field splitting term.

Simulations performed using a test case of S = 100, for which full simulation is possible, and its equivalent system with n= 10 are shown in Figure 3. The agreement between the two sets of simulations is rather good, with the exception of the low temperature spectrum in the parallel configuration especially in the low field region.

| | | |
|---|---|---|
| | 0.5 K | 25 K |

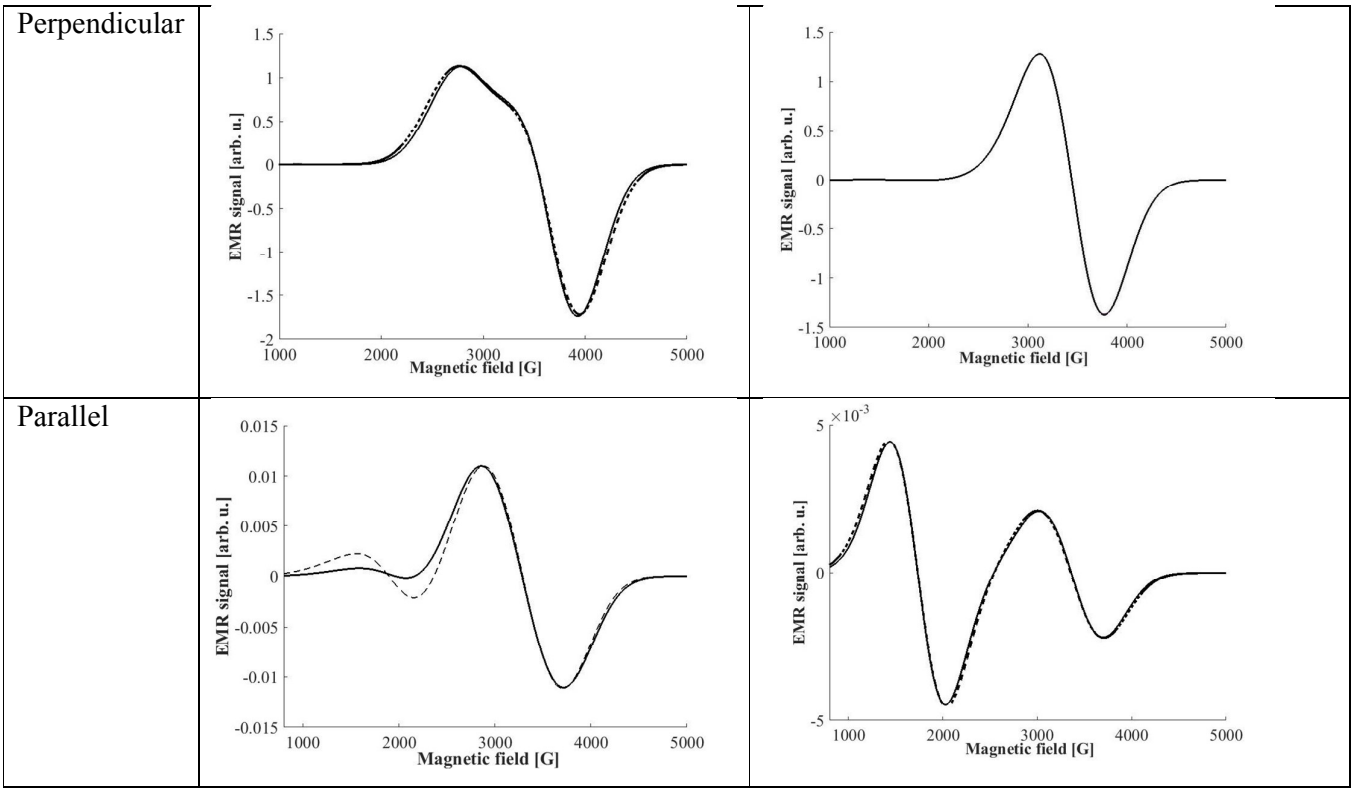


***Figure 3**: Full simulations are shown for the perpendicular and parallel configurations using a test case of S = 100, D = -10 MHz, T = 0.5 K and 25 K (continuous line) and the associated effective system $S_{eff}$ = 10, $D_{eff}$ = -100 MHz, $T_{eff}$ = 0.05 K and 2.5 K (dashed line).*

The above approach has been used to simulate the EMR spectra of ferritin MNPs for both parallel and perpendicular configurations. The best simulations of the EMR spectra were obtained using the parameters $S_{eff}$ = 10 and $D_{eff}$ =-100 MHz, which corresponds to a system of S =1000 and D = -1 MHz. However, a non isotropic distribution of the easy axes had to be used in order to reproduce the temperature dependence of the EMR spectra based on the function shown in Eq. 2,

$$P(\theta) = \sin(\theta)\,(\alpha+1)\cdot(\cos(\theta))^{\alpha} \qquad (2)$$

instead of the usual sin(θ) behaviour. This accounts for the powder-like pattern, in which α is a parameter depending on the temperature and θ is the direction between the easy axis of the ZFS tensor and the direction of the external magnetic field. In particular, Eq.2 and the α values used were such that upon lowering the temperature, the probability to find MNPs with the easy axes having an orientation perpendicular to the external magnetic field is gradually reduced. In order to introduce weighted contributions of each orientation to the total simulated spectrum, the θ interval 0°-90° was sampled every 2°. The spectra were simulated for each θ using Easyspin[27] and then

summed using Eq.2. In Figures 4 and 5, the comparison between the experimental and simulated spectra in both parallel and perpendicular configurations at various temperatures are shown.

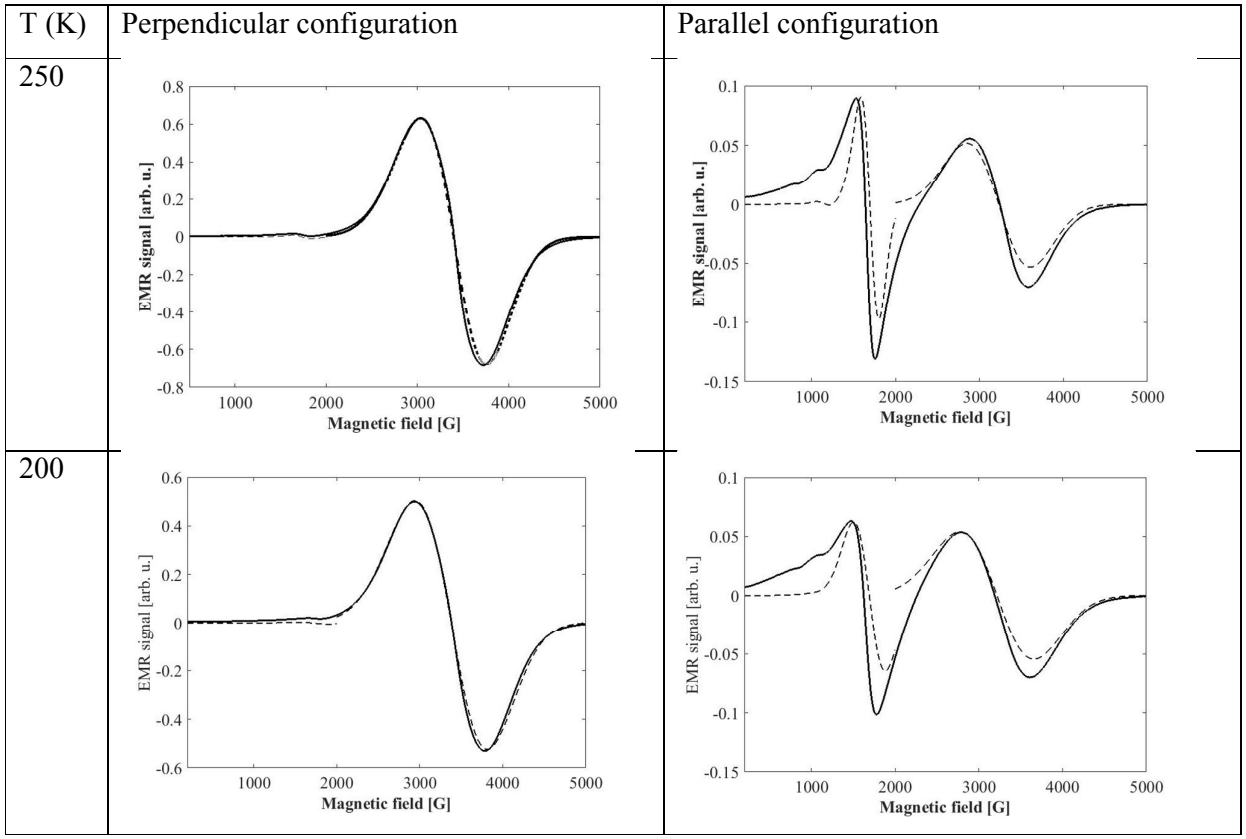


***Figure 4:*** *Experimental EMR spectra (continuous line) acquired in the parallel and perpendicular configurations at 250 K and 200 K, and simulations (dashed line) using* $S_{eff}$ *= 10, n = 100,* $D_{eff}$ *= -100 MHz. Different linewidths have been used for the field range 0-2000 G (20 MHz at 250 K and 40 MHz at 200 K) and the range 2000 G- 5000 G (75 MHz at 250 K and 92.5 MHz at 200 K). The value of* $\alpha$ *used was 0.7 for both temperatures.*

At 250 K and 200 K, the same $\alpha$ value could be used. The introduction of the parameter $\alpha$ is required to reproduce the spectral shape and cannot be eliminated by the use of a g value higher than 2.0023. The agreement between the experimental and simulated spectra is rather good in both measurement configurations. Even small features in the spectra recorded at 250 K in both configurations at low fields are well reproduced, such as the $\Delta M = \pm 3$ transitions observed in the parallel configuration at 250 K (Figure 4). Importantly, this underlines that the half field

contributions to the spectra, enhanced when the spectra are recorded in parallel configuration, derive from the whole system.

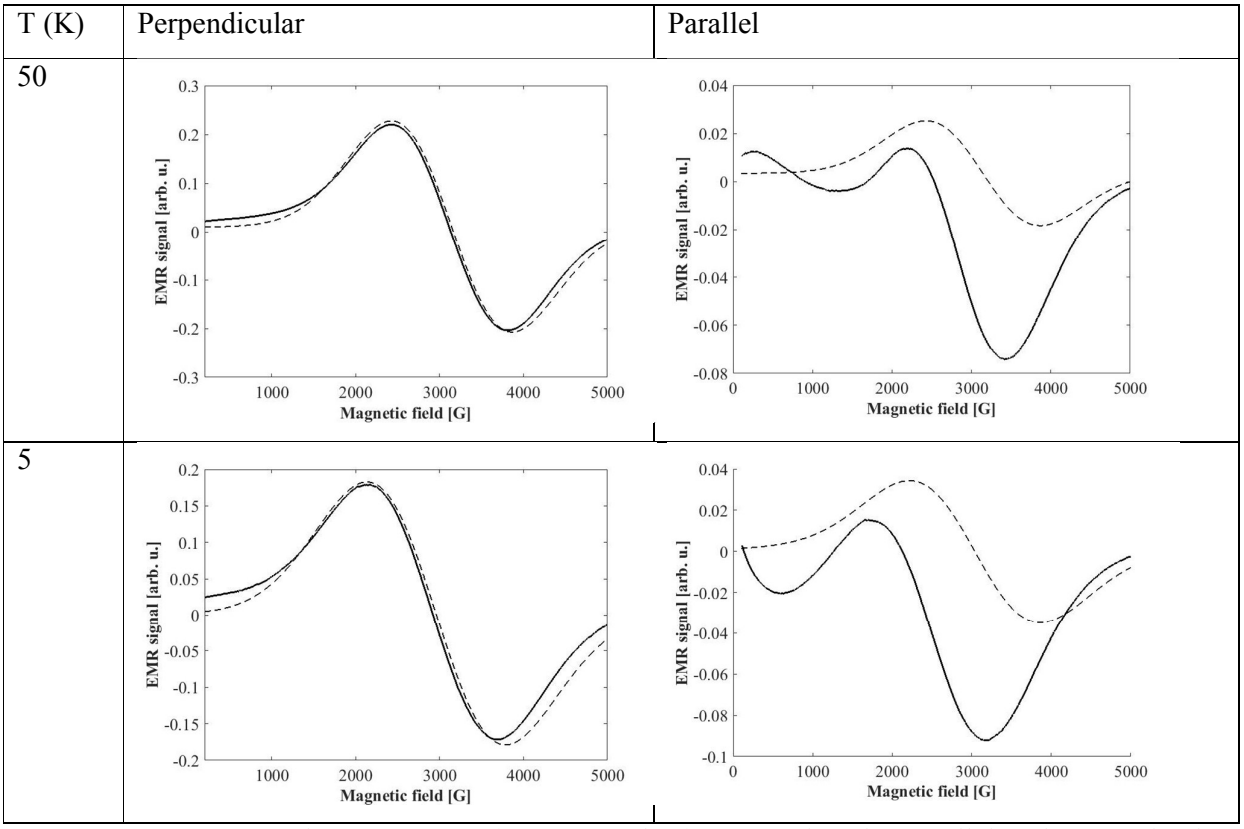


***Figure 5:*** *Experimental EMR spectra (continuous line) acquired in the parallel and perpendicular configurations at 50 K and 5 K, and simulations (dashed line) using* $S_{eff}$ *= 10, n = 100,* $D_{eff}$ *= -100 MHz. Linewidths used: 160 MHz for 50 K and190 MHz for 5 K. The value of* $\alpha$ *used was 2.1 for 50 K and 5 for 5 K.*

The agreement between experimental and simulated spectra at 50 K and 5 K is quite good in the perpendicular configuration, while it is poorer in the parallel configuration (Figure 5). To achieve the good agreement between experimental and simulated resonance fields in the perpendicular configuration at 5 K, the tendency of the simulated resonance field to be too high was countered by increasing the $\alpha$ parameter up to a value of 5. It appears that experimentally the contribution of the MNPs with easy axes perpendicular to the external magnetic field becomes less and less important.

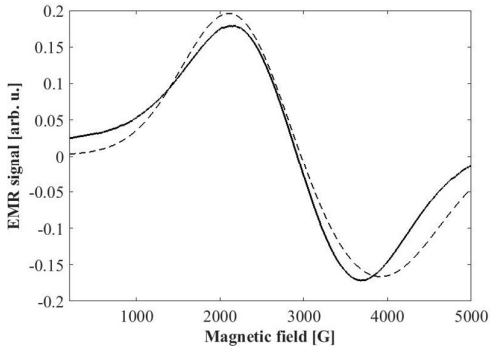


***Figure 6:*** *Experimental EMR spectrum (continuous line) acquired in the perpendicular configuration at 5 K, and its simulation (dashed line) using $S_{eff}$ = 10, n = 500 (S=5000) D = -0.34 MHz, linewidth 150 MHz, $T_{eff}$ = 0.01, and $\alpha$= 0.8.*

It should be noted that at 5 K it is not possible to distinguish between the simulations of a system with S = 1000, D = -1 MHz, $T_{eff}$ =0.05 K and a system with S= 5000, D = -0.2, MHz, $T_{eff}$ = 0.01 K, for the latter case the spin value corresponds to the that extracted from the magnetic data[16].

Notably, a simulation performed using $S_{eff}$ =10, D=-0.34 MHz, n = 500 (corresponding to S= 5000) gives good agreement at low temperature without the need of introducing such high $\alpha$ values (a value of 0.8 is sufficient), see Figure 6. However, this effective spin system does not give a good simulation of the EMR spectra at high temperatures. Hence, it is likely that the $\alpha$ parameter that we have to introduce is nothing other than a way to take into account that the population of the S states changes with temperature. Therefore, S = 5000 is closer to the value of the spin ground state of the system.

The poor correspondence between experimental and simulated spectra in the parallel configuration is due to i) the mixing between resonator modes, which cannot be properly controlled and therefore simulated, and ii) the effect of the disagreement of the model for the parallel configuration at low field, as noted above (see also Figure 3). The contribution of the first point is clearly present also at high temperatures, whereas the second effect is intrinsic and cannot be overcome here. It should be noted that the simulation with S = 5000 (n = 500) at 5 K in the parallel configuration is virtually unchanged compared to that obtained using S = 1000 (n = 1000).

In Table 1, the values of S and D of MNPs in ferritin, obtained from different types of measurements are reported: i) this work, ii) magnetic measurements, iii) previously obtained values from the orientation dependent EMR spectra acquired for a sample frozen in the presence of an external magnetic field.

***Table 1**: S and D values of MNPs in ferritin*

| Type of measurement | S | D (MHz) |
|---|---|---|
| EPR high temperature[a] | 1000 ($S_{eff}$ =10) | -1 |
| EPR low temperature[a] | 5000 ($S_{eff}$ =10) | -0.34 |
| Magnetic measurements[b] | 5000 | -0.40 |
| EPR sample frozen in presence of field[b] | | -0.14 (assuming S=5000) |
| EPR sample frozen in presence of field[b] | | -0.70 (assuming S=1000) |

[a]This work, [b] REF (16)

**Discussion**

EMR spectra of MNPs have been acquired extending the standard perpendicular mode configuration of the $B_1$ field of the microwave radiation with respect to the external magnetic field to include, for the first time, parallel mode configuration. All the EMR spectra have been interpreted in terms of a rather simple model based on the giant spin that can be associated with the whole MNP. In particular, an attempt to reproduce the EMR spectra of such huge spin values (of the order of thousands) using an equivalent smaller spin of the order of ten has been presented. The model represents a significant oversimplification of the system, which has the merit of elucidating better the physical properties of MNPs. It has to be noted that, since the two terms of the spin Hamiltonian (Eq.1) are of the same order, a perturbation approach could not be pursued.

At high temperature, by associating a spin value of 1000 to the MNP, a rather good agreement between the experimental and simulated spectra in both measurement configurations is obtained. This highlights that the half-field contributions to the spectra, enhanced when the spectra are recorded in parallel configuration, derive from the whole system. Therefore, it is imperative that these systems be considered and addressed as quantum objects.

In order to reproduce the EMR spectra also at low temperature, a temperature dependent parameter, $\alpha$, has to be introduced while maintaining the other spin Hamiltonian parameters fixed. On the other hand, this can be limited by using a different spin value equal to 5000. Therefore, the model indicates that the temperature dependence of the EMR spectra of MNPs is not only due to the thermal population of different M states of a fixed spin state S, as previously reported[28] but is far more complex and derives also from the thermal population of nearby excited S states. This behaviour can also be expected when these systems are compared with MNMs, as found for the

case of $Fe_{19}$. In this case, the thermal dependence of the EMR spectra enabled the energy separation ($E_g$ = 8 K) between the fundamental spin state level and the first excited spin state to be obtained. [25] The tendency for the $E_g$ value to become reduced upon increasing the size of the cluster has been also reported. [1,25,29,30]

The comparison of the findings of the quantum approach described herein with the classical model used in the past is instructive. A classical model had been used to analyze the thermal behaviour of the resonance position in the so-called strong field approximation ($B_0 >> B_a$) and uniaxial anisotropy by the relations

$$B_r = \frac{\omega_0}{\gamma} - \frac{B_a}{2}\frac{L_2}{L_1}(3cos^2\theta - 1), \quad (3)$$

where $L_2(x) = 1 - 3\frac{L_1(x)}{x}$, $L_1(x) = \coth x - \frac{1}{x}$ is the Langevin function, with $x = {}^{M_S VB}/_{k_B T} = {}^{\mu B}/_{k_B T}$, and $\theta$ is the angle between the external field and the easy axis of the considered MNP.

The total width of the EMR spectrum was described by

$$\Delta = \frac{3}{2}B_a^{eff} = \frac{3}{2}\frac{L_2(x)}{L_1(x)}. \quad (4)$$

We have also used this approach, however the agreement between the experimental and theoretical model was poor. [17] The approach described in this paper allows us to understand the reasons for the failure of the classical method to reproduce also the thermal trend of the main features of the EMR spectra acquired in the perpendicular configuration. Firstly, as we have already noted, the strong field approximation does not hold for these systems, secondly, the temperature behaviour of the EMR spectra depends critically on the effective population of spin states which cannot be obtained from the magnetization saturation value.

Notably, the spin ground state and anisotropy fields determined from the simulation of the 5 K EMR spectrum agree well with the value deduced from the saturation magnetization value obtained at 1.8 K (see Table 1). Indeed, the simulation of the EMR spectrum allows an independent estimation of the anisotropy field to be obtained. Conversely, at high temperatures, a spin state of 1000 is more appropriate to describe the system and the corresponding anisotropy field is closer to the value previously obtained for EMR spectra frozen in a magnetic field at a temperature of 200 K (Table 1).

In summary, the results presented herein demonstrate that it is possible to achieve a more thorough analysis of the properties of MNPs by using a simplified model based on the giant spin, in

which the spin is associated with the whole NMP and, consequently, the system must be treated as a quantum object. This approach can be used to characterize MNP in a semi-quantitative fashion.

**Acknowledgements**

We gratefully acknowledge financial support from the Fondazione CARIPLO. We are grateful to Dr. Barry Howes for careful reading of the manuscript.

References

1 M. Fittipaldi, L. Sorace, A. L. Barra, C. Sangregorio, R. Sessoli, and D. Gatteschi, *Phys.Chem.Chem.Phys.*, 2009, **11**, 6555

2 W. Wernsdorfer, *Adv.Chem.Phys.*, 2001, **118**, 99

3 A. H. Lu, E. L. Salabas, and F. Schuth, *Angew.Chem. Int. Ed.*, 2007, **46**, 1222

4 A. H. Lu, W. Schmidt, N. Matoussevitch, H. Bonnemann, B. Spliethoff, B. Tesche, E. Bill, W. Kiefer, and F. Schuth, *Angew.Chem. Int. Ed.*, 2004, **43**, 4303

5 T. Hyeon, *Chem.Comm.*, 2003, 927

6 *Nanomagnetism and Spintronics*, ed. T. Shinjo, Elsevier, Amsterdam, 2009,

7 S. Laurent, D. Forge, M. Port, A. Roch, C. Robic, L. V. Elst, and R. N. Muller, *Chem.Rev.*, 2008, **108**, 2064

8 *Magnetism in Medicine: A Handbook*, Wiley - VCH, Weinheim Germany, 2007,

9 S. Chikazumi, S. Taketomi, M. Ukita, M. Mizukami, H. Miyajima, M. Setogawa, and Y. Kurihara, *J.Magn.Magn.Mater.*, 1987, **65**, 245

10 A. K. Gupta and M. Gupta, *Biomaterials*, 2005, **26**, 3995

11 Q. A. Pankhurst, J. Connolly, S. K. Jones, and J. Dobson, *J.Phys.D-Appl.Phys.*, 2003, **36**, R167

12 D. W. Elliott and W. X. Zhang, *Environ.Sci.Technol.*, 2001, **35**, 4922

13 M. Takafuji, S. Ide, H. Ihara, and Z. H. Xu, *Chem.Mater.*, 2004, **16**, 1977

14 E. Fantechi, C. Innocenti, M. Zanardelli, M. Fittipaldi, E. Falvo, M. Carbo, V. Shullani, L. Cesare Mannelli, C. Ghelardini, A. M. Ferretti, A. Ponti, C. Sangregorio, and P. Ceci, *ACS Nano*, 1-4-2014, **8**, 4705

15 D. Gatteschi, M. Fittipaldi, C. Sangregorio, and L. Sorace, *Angew. Chem., Int. Ed.*, 2012, **51**, 4792

16 M. Fittipaldi, C. Innocenti, P. Ceci, C. Sangregorio, L. Castelli, L. Sorace, and D. Gatteschi, *Phys.Rev.B*, 17-3-2011, **83**, 104409

17 P. Ceci, E. Chiancone, O. Kasyutich, G. Bellapadrona, L. Castelli, M. Fittipaldi, D. Gatteschi, C. Innocenti, and C. Sangregorio, *Chem.,Eur.J.*, 2010, **16**, 709

18 N. Noginova, T. Weaver, E. P. Giannelis, A. B. Bourlinos, V. A. Atsarkin, and V. V. Demidov, *Phys.Rev.B*, 2008, **77**, 014403

19 A. L. Barra, L. C. Brunel, D. Gatteschi, L. Pardi, and R. Sessoli, *Acc.Chem.Res.*, 1998, **31**, 460

20 D. Gatteschi, A. L. Barra, A. Caneschi, A. Cornia, R. Sessoli, and L. Sorace, *Coord.Chem.Rev.*, 2006, **250**, 1514

21 McInnes, E. J. L., Spectroscopy of Single-molecule Magnets, ed. R. E. P. Winpenny, Springer, Berlin, 2006

22 R. S. Edwards, S. Maccagnano, E. C. Yang, S. Hill, W. Wernsdorfer, D. Hendrickson, and G. Christou, *J.Appl.Phys.*, 2003, **93**, 7807

23 S. Hill, S. Maccagnano, K. Park, R. M. Achey, J. M. North, and N. S. Dalal, *Phys.Rev.B*, 2002, **65**, 224410

24 R. H. Kodama and A. E. Berkowitz, *Phys.Rev.B*, 1999, **59**, 6321

25 L. Castelli, M. Fittipaldi, A. K. Powell, D. Gatteschi, and L. Sorace, *Dalton Trans.*, 2011, **40**, 8145

26 O. Kasyutich, A. Ilari, A. Fiorillo, D. Tatchev, A. Hoell, and P. Ceci, *J.Am.Chem.Soc.*, 2010, **132**, 3621

27 S. Stoll and A. Schweiger, *J.Magn.Reson.*, 2006, **178**, 42

28 N. Noginova, F. Chen, T. Weaver, E. P. Giannelis, A. B. Bourlinos, and V. A. Atsarkin, *J.Phys.-Condens.Mat.*, 2007, **19**, 246208

29 D. Zipse, J. M. North, N. S. Dalal, S. Hill, and R. S. Edwards, *Phys.Rev.B*, 2003, **68**, 1844081

30 L. Sorace, M. E. Boulon, P. Totaro, A. Cornia, J. Fernandes-Soares, and R. Sessoli, *Phys.Rev.B*, 2013, **88**, 104407